

## Simulation study on non-linear effects of initial melt temperatures on microstructures during solidification process of liquid Mg<sub>7</sub>Zn<sub>3</sub> alloy

Rang-su LIU<sup>1</sup>, Yong-chao LIANG<sup>1</sup>, Hai-rong LIU<sup>2</sup>, Nai-chao ZHENG<sup>2</sup>, Yun-fei MO<sup>1</sup>  
Zhao-yang HOU<sup>3</sup>, Li-li ZHOU<sup>4</sup>, Ping PENG<sup>2</sup>

1. School of Physics and Microelectronics Science, Hunan University, Changsha 410082, China;
2. College of Materials Science and Engineering, Hunan University, Changsha 410082, China;
3. Department of Applied Physics, Chang'an University, Xi'an 710064, China;
4. Department of Information Engineering, Gannan Medical University, Ganzhou 341000, China

Received 27 June 2012; accepted 5 December 2012

**Abstract:** The non-linear effects of different initial melt temperatures on the microstructure evolution during the solidification process of liquid Mg<sub>7</sub>Zn<sub>3</sub> alloys were investigated by molecular dynamics simulation. The microstructure transformation mechanisms were analyzed by several methods. The system was found to be solidified into amorphous structures from different initial melt temperatures at the same cooling rate of  $1 \times 10^{12}$  K/s, and the 1551 bond-type and the icosahedron basic cluster (12 0 12 0) played a key role in the microstructure transition. Different initial melt temperatures had significant effects on the final microstructures. These effects only can be clearly observed below the glass transition temperature  $T_g$ ; and these effects are non-linearly related to the initial melt temperatures, and fluctuated in a certain range. However, the changes of the average atomic energy of the systems are still linearly related with the initial melt temperatures, namely, the higher the initial melt temperature is, the more stable the amorphous structure is and the stronger the glass forming ability will be.

**Key words:** liquid Mg–Zn alloy; initial melt temperature; microstructure evolution; molecular dynamics simulation; cluster-type index method

### 1 Introduction

For the solidification of liquid metals, many studies are available on the effect of such thermal history conditions with initial melt temperature on the solidification structure and property of metals [1–7]. GUIMBARD and GOBIN [1] examined the effect of the initial melt temperature on the hardness of the solidification structure of liquid metal Al. MANOV et al [2] studied the effect of the initial temperature on such physical properties as density, thermal expansion coefficient and resistance of amorphous alloys of Fe–B and Pd–Si. WEN et al [3] investigated the effect of melt quenching temperature on the recovery stress of shape memory alloy Fe–Mn–Si–Cr–Ni. TAKAYAMA and OI [4] studied the effect of different quenching temperatures on the magnetic performance of Fe–Ni–B alloys. BIAN et al [5] explored the effect of different melt casting temperatures on the amorphous critical thickness of

Al–Ni–Ce alloy by thermal rate treatment. CAO et al [6] studied the free-volume evolution and its temperature dependence during rolling of Cu<sub>60</sub>Zr<sub>20</sub>Ti<sub>20</sub> bulk metallic glass. ZHAO et al [7] researched the effect of thermal history on the crystal structures of fine Co particles of different sizes obtained by laser pyrolysis. However, a deep understanding in the microscopic mechanisms for above experimental results is still necessary for giving a more reasonable explanation. At present, the effect of the thermal history conditions such as initial melt temperatures on the solidification processes and microstructures of liquid metals will be investigated in depth at atomic level.

With rapid development of computer technology, it is now possible to employ molecular dynamics (MD) method with explicit physical concepts and images to study the solidification process and microstructure evolution mechanism of liquid metals. WANG et al [8] examined the change of medium-range order structure during the solidification process of liquid Cu<sub>3</sub>Au alloy

quenched from two different initial temperatures by MD method, and believed that the ordering degree of solidification microstructure increased with decrease in the initial temperature. LIU et al [9,10] also studied the effects of different initial temperatures and different heat preservation times on the microstructure evolution during the rapid solidification process of liquid metals Na and Al, and found that thermal history had a significant effect on the microstructure transition, and the effects were fully demonstrated below the glass transition temperature  $T_g$ .

On the basis of our previous works [9,10], in this study, a deep investigation on the solidification process of liquid  $Mg_7Zn_3$  alloy was made for 6 different initial melt temperatures (with the same cooling rate of  $1 \times 10^{12}$  K/s) by MD simulation. The effect of the initial melt temperature on the microstructure evolution and its mechanism during the solidification process were analyzed by adopting the Honeycutt-Andersen (HA) [11] bond-type index method, cluster-type index method (CTIM) [12–14] and average coordination numbers. Some new results were obtained that the effects of initial melt temperatures on the microstructure evolution were non-linearly related, and fluctuated in a certain range.

## 2 Simulation conditions and methods

The MD simulations were performed with a system containing 10000 atoms (7000 Mg atoms and 3000 Zn atoms) in a cubic box with periodic boundary conditions in  $NVT$  ensemble (in the  $NVT$  ensemble, the number of atoms, the volume of the space, and the average kinetic energy (temperature) remain constant). Interactions among atoms were calculated using the effective pair potential function of the generalized nonlocal model-pseudopotential (GNMP) theory developed by WANG et al [15,16], which can be defined as

$$V(r) = (Z_{\text{eff}}^2/r) \left[ 1 - \left( \frac{2}{\pi} \right) \int_0^\infty dq F(q) \sin(rq) / q \right] \quad (1)$$

where  $Z_{\text{eff}}$  is the effective ionic valence and  $F(q)$  is the normalized energy wave number characteristic. Both of them are defined in detail in Refs. [15,16]. The pair potential is cut off at 20 a.u. (atomic unit). The time step is  $10^{-15}$  s.

The initial melt temperatures of the simulation calculations were 1273, 1173, 1073, 973, 873 and 773 K, respectively (the melting point of  $Mg_7Zn_3$  alloy is around 670 K [17,18]), with the cooling rate of  $1 \times 10^{12}$  K/s. The systems run 20000 time steps at the same temperature to obtain an equilibrium state. In order to detect the microstructure evolution in the systems during the cooling processes, the systems run isothermally for 400

time steps after each decrease of 50 K, and the space coordinates of each atom in the systems and other relevant data were recorded. The pair distribution function  $g(r)$ , HA bond-type index method, cluster-type index method, average coordination number and average atomic energy were used to analyze these data, so as to explore the microstructure transition and evolution in the system at the atomic level.

## 3 Simulation results and analysis

### 3.1 Pair distribution function analysis

It is well known that the pair distribution function (PDF)  $g(r)$  is an important method to describe the statistical distributions of atoms in the system. Since PDF  $g(r)$  can be obtained by Fourier transformation of the structure factor  $S(q)$  of X-ray diffraction in a system, it is widely used to verify the validity of simulation by comparing the theoretical results with the experimental ones of the same system.

At present, the  $g(r)$  curves at 273 K obtained by calculation were transformed to  $S(q)$  and compared with the X-ray diffraction experimental results of RUDIN et al [18], as shown in Fig. 1. It can be seen that the simulation result is in good agreement with the experimental result both for the position of peaks and the change tendency, especially the splitting of the second peaks. This reveals that the effective pair potential function adopted here is rather successful for reflecting the objective physical nature of microstructure of this system.

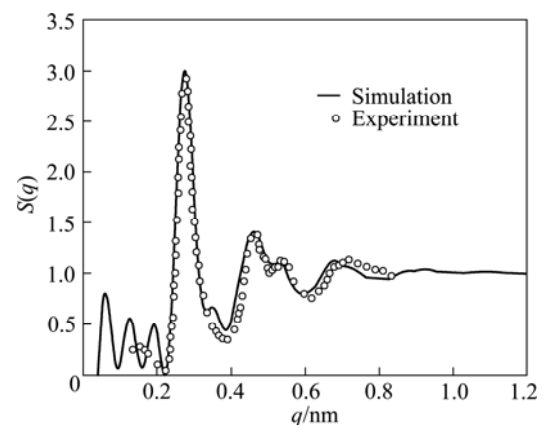


**Fig. 1** Comparison of structure factor of  $S(q)$  calculated at 273 K with experimental result of Ref. [18]

For better understanding of the PDF  $g(r)$  curves of this simulation of  $Mg-Zn$  alloy system, the curves of the three partial PDFs  $g_{Zn-Zn}(r)$ ,  $g_{Mg-Zn}(r)$  and  $g_{Mg-Mg}(r)$  and the total PDF  $g_{\text{tot}}(r)$  at different temperatures during the solidification process from the initial melt temperature of 1273 K are shown in Fig. 2. It can be seen that the two

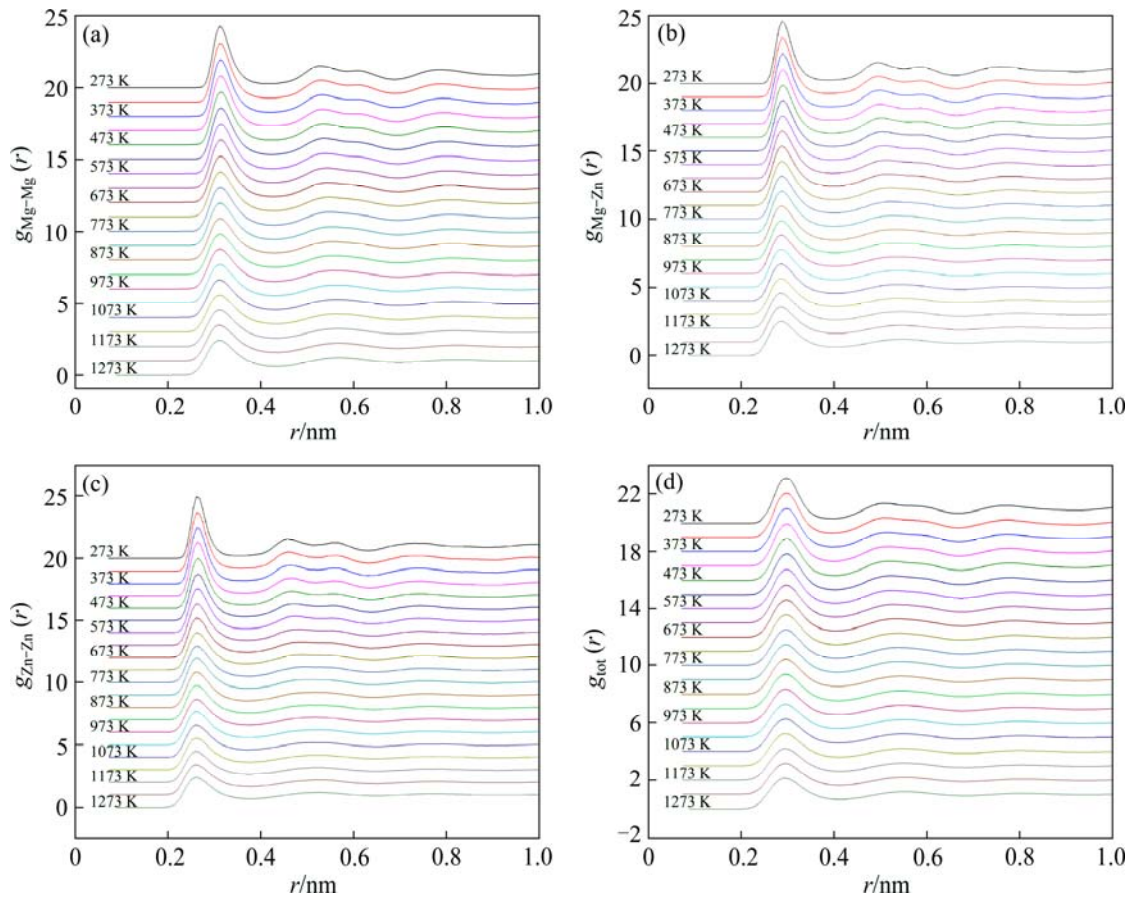


**Fig. 2** Whole pair distribution function  $g(r)$  curves at different temperatures during solidification process from initial melt temperature of 1273 K

secondary peaks at the second peak of the total PDF  $g_{\text{tot}}(r)$  curve do not appear as the same as those in three partial PDFs. This is exactly an important characteristic of the alloy system in the amorphous state, and it is significantly different from the single metal system [19–21].

For the evolution of other three partial PDFs in the alloy system, Fig. 2 shows that, with the decrease of temperature, the first peaks of  $g_{\text{Zn-Zn}}(r)$ ,  $g_{\text{Mg-Zn}}(r)$  and  $g_{\text{Mg-Mg}}(r)$  become sharp and high, indicating an increasing probability of forming bonds between neighboring atoms in the systems, and an increasing short-range order (SRO). The first peaks of  $g_{\text{Zn-Zn}}(r)$  curves are the highest and sharpest, suggesting that the probability of forming Zn–Zn bonds is the highest because the atomic radius of Zn is smaller than that of Mg. At 273 K, all the second peaks of  $g_{\text{part}}(r)$  are split to two obvious secondary peaks, which is just an important characteristic of amorphous structure. However, for the total PDF  $g_{\text{tot}}(r)$ , with the decrease of temperature, the first peak becomes higher, and the second peak becomes wider, shifts closer to the first peak, becomes more asymmetric, and begins to split at 523 K, finally two secondary peaks form, but far less significant than those

of  $g_{\text{part}}(r)$ . The reason for this, just according to Ref. [22], is that the 3-dimensional information of all  $g_{\text{part}}(r)$  of atoms is averaged in the  $g_{\text{tot}}(r)$  demonstrated by TANAKA [23] through comparison of the triple distribution function  $g(r_1, r_2, r_3)$  with the  $g_{\text{tot}}(r)$ . A further analysis of the  $g_{\text{tot}}(r)$  with Wendt-Abraham ratio  $R = g(r)_{\text{min}}/g(r)_{\text{max}}$  [24] reveals the glass transition temperature  $T_g$  being around 523 K, as shown in Fig. 3.

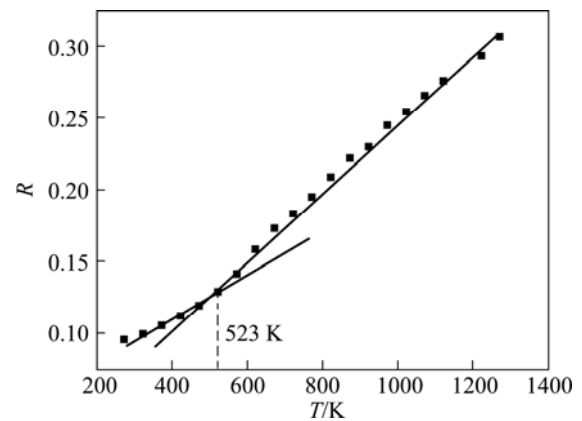


**Fig. 3** Relation of Wendt-Abraham ratio  $R$  with temperature during rapid solidification from initial melt temperature of 1273 K

Figure 4 shows the  $g(r)$  curves of the system cooled to 273 K from six different initial temperatures, in which all the second peaks are split, implying that the amorphous transition occurs in all cases. There are no significant differences in  $g(r)$  curves with different initial conditions, which, nevertheless, do not necessarily indicate that different initial conditions have no effect on the whole solidification process. A further analysis by HA bond-type index method and cluster-type index method is required to obtain a better understanding.

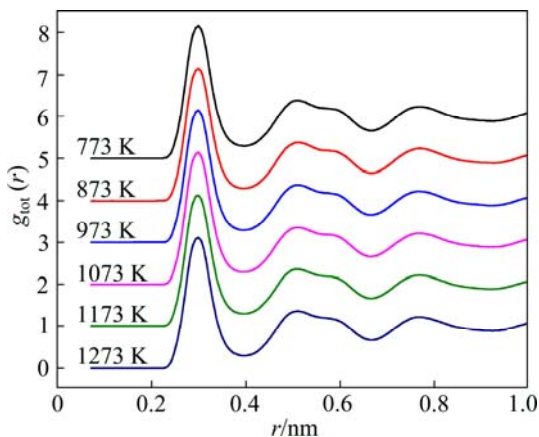


Fig. 4 PDF  $g_{\text{tot}}(r)$  curves of alloy cooled to 273 K from six different initial melt temperatures

### 3.2 Bond-type index analysis

Although the pair distribution function  $g(r)$  can reflect qualitatively the microstructure characteristic of the system, for a deep understanding of the relationship of an atom with its neighbors, it is necessary to quantitatively describe the local configurations of the system. At present, the HA bond-type index method is important and widely used to describe and analyze the microstructure transitions in liquid and amorphous systems as well as some crystallization systems. When the local configurations are described by the HA bond-type index method, it is well known that the 1551, 1541 and 1431 bond-types are the characteristic bond-types of typical liquid and amorphous states, whereas for various crystal structures, 1661 and 1441 (6:8) are the characteristic bond-types of BCC structure, and 1421 and 1422 are the characteristic bond-types of FCC (12:0) and HCP (6:6) structures.

For convenience, first of all we only give the relations of the relative numbers of the main bond-types with the temperature for the system solidified from the initial temperature of 1273 K, as shown in Fig. 5. It can be seen that the bond-types of 1551, 1541 and 1431 related to the icosahedron or defective icosahedron structures are the dominant ones in the system. These three bond-types account for more than 45% at 1273 K, and increase to above 75% at 273 K. The other

bond-types only change a little and decline, except that 1661 bond-type increases slightly.

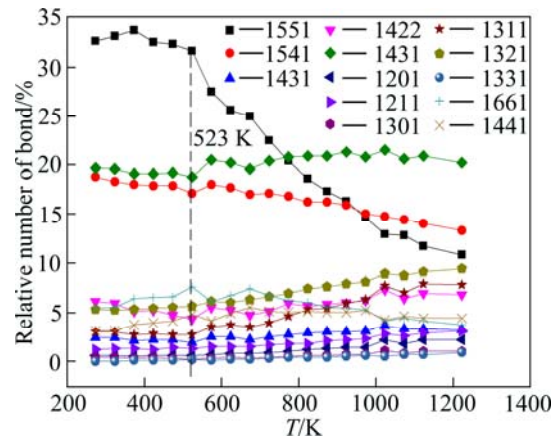


Fig. 5 Relations of relative numbers of main bond-types with temperature for initial melt temperature of 1273 K

It is found that only the 1551 bond-type increases gradually during the whole solidification process and is regarded as the characteristic bond-type in the system. It changes abruptly around 523–573 K, close to the glass transition temperature  $T_g$  as above-mentioned. In some of our previous works on pure metals Al [13], Cu [25], Pb [26,27] and alloys Al–Mg [28], Ca–Mg [21], similar results were obtained. All these indicate that the abrupt change point of the characteristic bond-type may be a new way to determine the glass transition temperature  $T_g$ .

Figure 6 shows the changes of the 1551 bond-types with the temperature for six different initial melt temperatures. It can be seen that, with the decrease of temperature, all the 1551 bond-types increase greatly, and change abruptly around the glass transition temperature  $T_g$ . All the 1551 bond-type curves are intersected at a point around 573 K, which is close to the  $T_g$  of 523 K, during the solidification processes from various initial temperatures. The reason for the

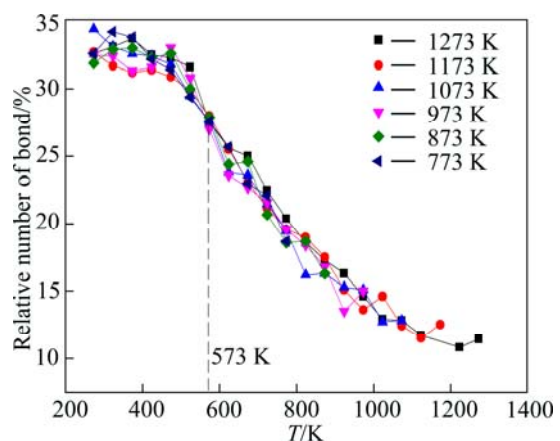


Fig. 6 Relations of 1551 bond-type with temperature for different initial melt temperatures

intersected point of 573 K will be studied in depth in the future. However, all the final numbers of 1551 bond-types are not linearly corresponded to the initial melt temperatures, and fluctuated in a certain range, namely, the final numbers of 1551 bond-types are nonlinearly related to the initial melt temperatures.

### 3.3 Cluster-type index analysis

However, the HA bond-type indices cannot describe and discern the different atomic clusters formed by an atom with its nearest neighbors. In order to describe various atomic clusters in the system, the cluster-type index method (CTIM) based on the work of QI and WANG [29] was proposed by LIU et al [12–14].

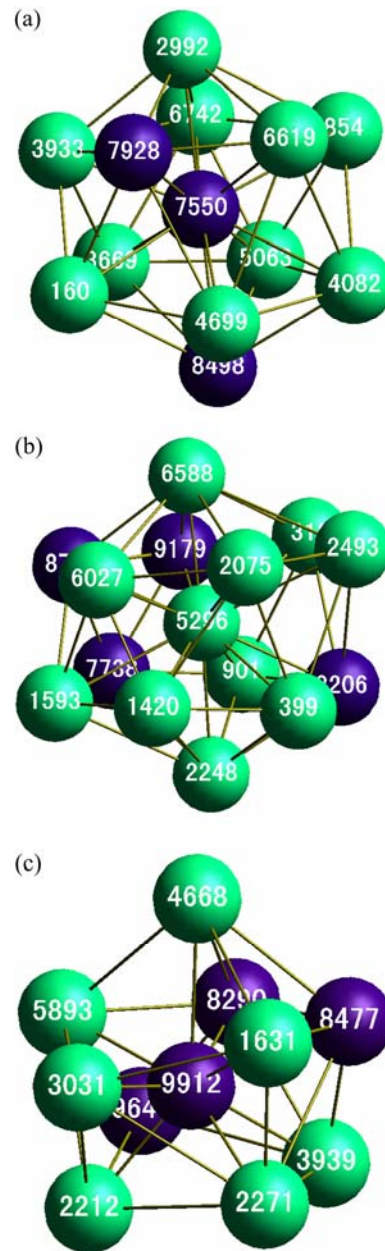
In the CTIM, four integers were used to describe a basic cluster. The first integer denotes the total number of surrounding atoms (i.e. the coordination number) which form a cluster along with the central atom. The second, third and fourth integers represent, respectively, the numbers of 1441, 1551 and 1661 bond-types by which the surrounding atoms are connected with the central atom. For example, the icosahedron basic cluster can be expressed by (12 0 12 0), Frank-Kasper polyhedron cluster can be expressed by (14 0 12 2), Bernal polyhedron cluster can be expressed by (10 2 8 0), and BCC basic cluster can be expressed by (14 6 0 8). Three basic clusters are selected in this simulation system, as shown in Fig. 7.

The CTIM used to analyze the relations of the number of main basic clusters in the system with temperature during the cooling process from different initial melt temperatures. The results for the initial temperature of 1273 K are shown in Fig. 8. It can be clearly seen that, at the higher initial temperature, a few clusters are still in the system. With the decrease of the temperature, the numbers of various clusters have different changes during the whole solidification process, of which the icosahedron basic cluster (12 0 12 0) increase most rapidly, followed by the basic clusters of (13 1 10 2), (15 1 10 4), (11 2 5 1).

The number of the icosahedron cluster (12 0 12 0) also has an abrupt change around 523–573 K, corresponding to the change of the 1551 bond-type in the bond-type index analysis and close to the glass transition temperature  $T_g$  mentioned above.

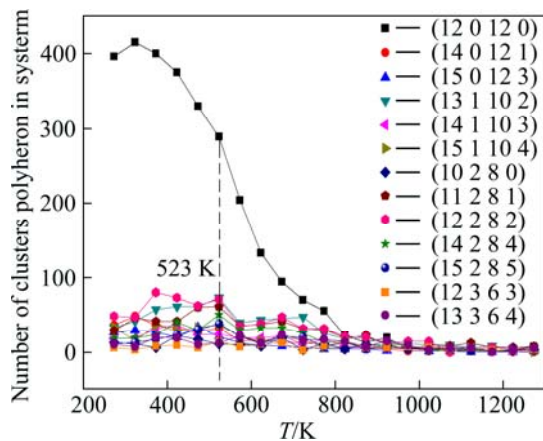
Similar results also can be found for the changes of the number of basic clusters with temperature under other initial conditions. For convenience only the change of the number of icosahedron clusters (12 0 12 0) for six different initial temperatures is shown in Fig. 9.

Figure 9 shows that all the number of icosahedron clusters (12 0 12 0) increases slowly at a higher temperature, with very close increase rates. However, at



**Fig. 7** Three basic clusters in system: (a) Icosahedron basic cluster (12 0 12 0) with central atom of 7550; (b) Frank-Kasper polyhedron cluster (14 0 12 2) with central atom of 5296; (c) Bernal polyhedron cluster (10 2 8 0) with central atom of 9912 (the light colored balls indicate Mg atoms, and the dark colored balls indicate Zn atoms.)

the glass transition temperature  $T_g$  of 523 K, the increase rates are quite different from each other. The icosahedron clusters (12 0 12 0) curves with different initial conditions are also almost intersected in a point about 573 K, close to  $T_g$ . The last number of icosahedron clusters (12 0 12 0) is also fluctuated in a certain range and they are nonlinearly related to the initial melt temperature as mentioned above for bond-type analysis.



**Fig. 8** Relations of number of main basic clusters with temperature during solidification from initial temperature of 1273 K

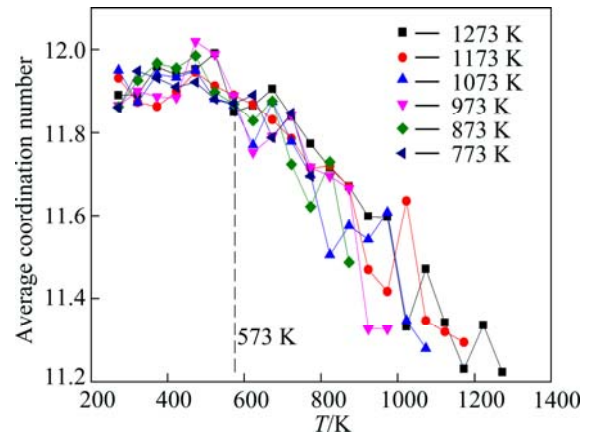


**Fig. 10** Relations of average coordination number with temperature during solidification processes from different initial temperatures

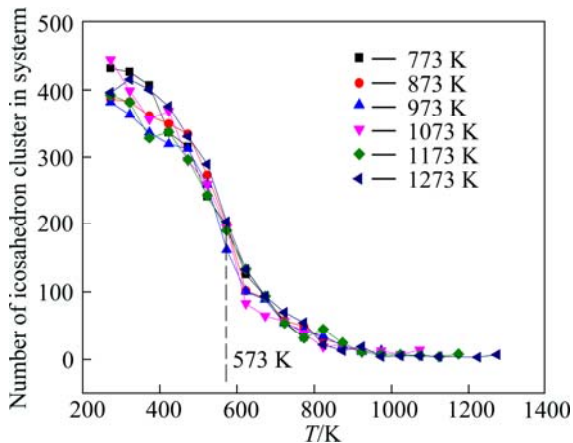


**Fig. 9** Relations of number of icosahedron clusters (12 0 12 0) with temperature for different initial temperatures

### 3.4 Average coordination number analysis

Average coordination number (ACN) is originally defined as the average number of neighboring atoms surrounding any atom in crystal structure. It is one of the most essential parameters to characterize the structure. The temperature at which an abrupt change of the ACN occurs usually corresponds to the structure transition temperature of crystals. For the liquid and amorphous structures, the ACN can also reflect the microstructure evolution in the system during the solidification process, providing a new method for research on the transition process of liquid and amorphous structures. The changes of the ACNs with temperature during the solidification process from different initial temperatures are given in Fig. 10.

Figure 10 shows that the ACNs of all systems increased with the decrease of temperature, ultimately approaching 12. This suggests that a dominant number of icosahedron basic clusters with the coordination number of 12 are formed during the formation of amorphous

structures, which is in agreement with the previous discussion. However, the coordination numbers for different initial melt temperatures is all less than 12, which exactly demonstrates that a considerable number of atoms were in basic clusters with the coordination number less than 12. The curves of the ACNs for different initial temperatures almost intersect at the same point of 573 K, after which the ACNs increase or decrease at different rates. The last values are different and also nonlinearly related to the initial melt temperatures. This is consistent with previous analyses.

The change of the ACN with the temperature for different initial temperatures in this study is significant. The relation of the initial ACN with different initial temperatures is plotted as shown in Fig. 11, it can be seen that this relation curve is consistent with the change tendency of the coordination number with the temperature for Al–Ni–Ce alloy under different casting temperatures as shown in Fig. 10 in Ref. [5].

### 3.5 Average atomic energy analysis

The relations between the average atomic energies (AAE) and the temperature during the solidification processes from different initial temperatures are given in Fig. 12. It can be found that the AAE for different initial conditions all decrease with the decrease of the temperature. No abrupt decline is observed, indicating that no crystallization occurs during the solidification from these initial conditions, and amorphous structures are formed in all systems, which agrees well with the previous analyses [27,30].

Figure 12 shows that the temperatures corresponding to the maximum slopes on the change curves of the AAE, namely, the turning points of slopes, are around 523–573K, close to the glass transition

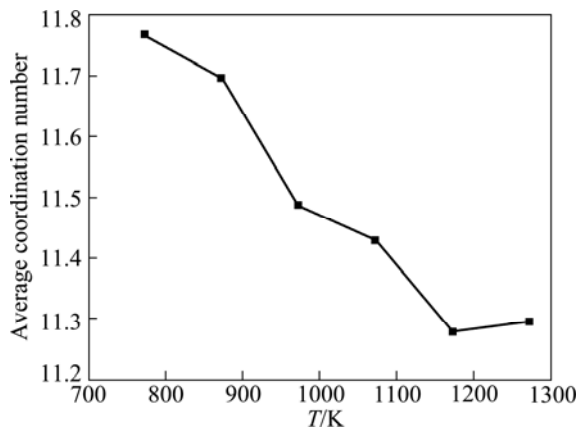


**Fig. 11** Relation of initial average coordination number with different initial melt temperatures

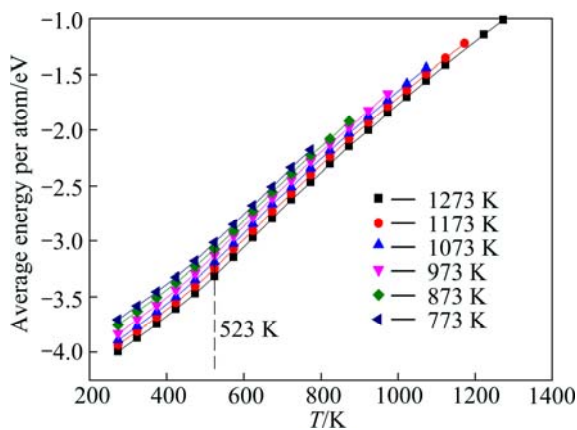


**Fig. 12** Relations of average atomic energies with temperature during solidification process from different initial temperatures

temperature  $T_g$  as mentioned above. It can also be found that, the higher the initial temperature is, the lower the AAE is, so that the higher the SRO of the system is, and the more stable the amorphous structure formed is, namely, the higher the initial temperature is, the stronger the amorphous forming ability of the system is, thus the thicker the amorphous band is at the same cooling rate. This is in good agreement with the experimental result obtained in Ref. [5].

From what mentioned above, it is found that the final values of the main bond-types, main basic clusters and average coordination numbers are all nonlinearly related to the initial melt temperatures. This is different from the results in Ref. [8] that the ordering degree of solidification structure increases linearly with the decrease of the initial temperature. The reason for this may be because only two different initial temperatures were considered in Ref. [8], and the nonlinear relation was not observed. A further analysis of the above nonlinear relations reveals that this nonlinear relation fluctuates in a certain range and the fluctuation range becomes narrower with the decrease of the initial

temperature. Although it is impossible to determine the minimum fluctuation range because the initial temperatures studied are limited. It is apparent that the fluctuation has upper and lower limits. The existence of upper and lower limits of the nonlinear relations concerning the effect of the initial temperature on the solidification microstructures makes it more difficult to find the optimum initial temperature to obtain the optimized solidification structure. However, it indicates that the solidification microstructure can be controlled by changing the initial temperature.

Reason for the nonlinear relation between the thermal history and the solidification microstructure, and for the existence of the upper and lower limits for the degree of effect. No one does not find reasonable explanation available yet. The authors of this study believe that the whole one especially the rapid solidification process, is a typical nonlinear, non-equilibrium thermodynamic process. The various microstructures and clusters of different types formed during the solidification process are just the “dissipative structures” in the theory of the dissipative structures proposed by NICOLIS and PRIGOGINE [31], which are formed under the “nonlinear” interaction among various atoms and microstructures in the system when the system is far from equilibrium. The “nonlinear” characteristic of the interaction between various atoms and microstructures in the system is mainly a result of the combined effect of the contingency of thermal fluctuation in system and the randomness of dynamics during interaction. The action mechanism is very complicated with no linear correlation. However, from the view point of thermodynamic fluctuation, the extents of thermal fluctuations are different for melts with different initial temperatures. Generally, the higher the initial melt temperature is, the wider the variation range of the thermal fluctuation is, and the greater the energy change induced by thermal fluctuation is. Because of the randomness of dynamics during interaction, the system is actually in any random state in the change range caused by the thermal fluctuation, namely, with the upper and lower limits, but not in the statistically averaged state that the system may have. Accordingly, the upper and lower limits of the degree of effect of the thermal history on the structural state can be explained qualitatively. As for the specific action mechanism of this effect, a further in-depth investigation is required in the future.

## 4 Conclusions

1) When liquid Mg–Zn alloys are cooled rapidly from six initial melt temperatures with the same rate of  $1 \times 10^{12}$  K/s, the systems are all solidified into amorphous structures. The icosahedron cluster (12 0 12 0) and the

1551 bond-type play a key role in the microstructure transition during the whole solidification process.

2) During the solidification process of liquid Mg–Zn alloys, the important effects of different initial temperatures on the microstructures can be fully demonstrated only below the amorphous transition temperature  $T_g$ .

3) Different initial melt temperatures have different degrees of effects on the amorphous characteristics of the solidification structures, such as the 1551 bond-type, icosahedron cluster (12 0 12 0) and average coordination number. The degrees of effects are nonlinearly related to the initial melt temperatures and fluctuated in a certain range, and the fluctuation range decreases gradually with the decline of the initial temperature, and can be controlled.

4) The change of average atomic energy (AAE) is linearly related to the initial melt temperature. The higher the initial temperature is, the lower the AAE of the amorphous structure finally formed is, that is, the more stable the amorphous structure is, and the stronger the amorphous forming ability is. This is conducive to a deeper investigation on the microstructure transition mechanism during the solidification process of liquid metals.

## References

- [1] GUIMBARD J, GOBIN P. The influence of quenching temperature on the hardening of pure aluminium quenched to  $-72\text{ }^{\circ}\text{C}$  [J]. *British Journal of Applied Physics*, 1967, 18: 1641–1644.
- [2] MANOV V P, POPEL S I, BULER P I, MANUKHIN A B, KOMLEV D G. The influence of quenching temperature on the structure and properties of amorphous alloys [J]. *Materials Science and Engineering A*, 1991, 133: 535–540.
- [3] WEN Y H, LI N, TU M J. Effect of quenching temperature on recovery stress of Fe–18Mn–5Si–8Cr–4Ni alloy [J]. *Scripta Mater*, 2001, 44: 1113–1116.
- [4] TAKAYAMA S, OI T. The effects of processing conditions on magnetic properties of amorphous alloys [J]. *Journal of Applied Physics*, 1979, 50: 1595–1597.
- [5] BIAN X F, SUN M H, XUE X Y, QIN X B. Medium-range order and viscosity of molten Cu–23%Sn alloy [J]. *Materials Letters*, 2003, 57: 2001–2006.
- [6] CAO Q P, LI J F, ZHOU Y H. Free-volume evolution and its temperature dependence during rolling of Cu<sub>60</sub>Zr<sub>20</sub>Ti<sub>20</sub> bulk metallic glass [J]. *Applied Physics Letters*, 2005, 87(10): 101901.
- [7] ZHAO X Q, VEINTEMILLAS-VERDAGUER S, BOMATI-MIGUEL O, MORALES M P, XU H B. Thermal history dependence of the crystal structure of Co fine particles [J]. *Physical Review B*, 2005, 71: 024106–024113.
- [8] WANG L, CONG H R, ZHANG Y N, BIAN X F. Medium-range order of liquid metal in the quenched state [J]. *Physica B*, 2005, 355: 140–146.
- [9] LIU Rang-su, LIU Feng-xiang, LI Ji-yong, DONG Ke-jun, ZHENG Cai-xing. Effects of thermal history of liquid metal Al on its solidification microstructures [J]. *Acta Physico-Chimica Sinica*, 2003, 19(9): 791–794. (in Chinese)
- [10] HOU Zhao-yang, LIU Rang-shu, WANG Xin, TIAN Ze-an, ZHOU Qun-yi, CHEN Zhen-hua. Simulation study of effects of initial melt temperature on microstructure of liquid metal Na during solidification processes [J]. *Acta Physica Sinica*, 2007, 56: 376–383. (in Chinese)
- [11] HONEYCUT J D, ANDERSEN H C. Molecular dynamics study of melting and freezing of small lennard-jones clusters [J]. *Journal of Protein Chemistry*, 1987, 91: 4950–4963.
- [12] LIU R S, DONG K J, LI J Y, YU A B, ZOU R P. Formation and description of nano-clusters formed during rapid solidification processes in liquid metals [J]. *Journal of Non-Crystalline Solids*, 2005, 351: 612–617.
- [13] LIU R S, DONG K J, TIAN Z A, LIU H R, PENG P, YU A B. Formation and magic number characteristics of clusters formed during solidification processes [J]. *Journal of Physics: Condensed Matter*, 2007, 19: 196103–196120.
- [14] LIU R S, LIU H R, DONG K J, HOU Z Y, TIAN Z A, PENG P, YU A B. Simulation study of size distributions and magic number sequences of clusters during the solidification process in liquid metal Na [J]. *Journal of Non-Crystalline Solids*, 2009, 355: 541–547.
- [15] WANG S, LAI S K. Structure and electrical resistivities of liquid binary alloys [J]. *Journal of Physics F: Metal Physics*, 1980, 10: 2717–2737.
- [16] LI D H, LI X R, WANG S. Variational calculation of Helmholtz free energies with applications to the sp-type liquid metals [J]. *Journal of Physics F: Metal Physics*, 1986, 16: 309–321.
- [17] SUCH J B, RUDIN H, GUNTHERODT H J, BECK H. Influence of structural relaxation on the atomic dynamics of the metallic glass Mg<sub>70</sub>Zn<sub>30</sub> [J]. *Journal of Non-Crystalline Solids*, 1984, 61–62: 295–301.
- [18] RUDIN H, JOST S, GUNTHERODT H J. X-ray diffraction from liquid and amorphous Mg<sub>70</sub>Zn<sub>30</sub> alloys [J]. *Journal of Non-Crystalline Solids*, 1984, 61–62: 291–294.
- [19] LIU Rang-su, QIN Shu-ping, HOU Zhao-yang, CHEN Xiao-ying, LIU Feng-xiang. Simulation study of microstructure transition of liquid metal in during solidification processes [J]. *Acta Physica Sinica*, 2004, 53(9): 3119–3124. (in Chinese)
- [20] HOU Zhao-yang, LIU Li-xia, LIU Rang-su, TIAN Ze-an. Simulation of evolution mechanisms of microstructures during rapid solidification of Al–Mg alloy melt [J]. *Acta Physica Sinica*, 2009, 58(7): 4817–4825. (in Chinese)
- [21] GAO Ting-hong, LIU Rang-su, ZHOU Li-li, TIAN Ze-an, XIE Quan. Formation properties of cluster structures during the rapid solidification of liquid Ca<sub>7</sub>Mg<sub>3</sub> alloy [J]. *Acta Physico-Chimica Sinica*, 2009, 25(10): 2093–2010. (in Chinese)
- [22] LI D H, MOORE R A, WANG S. A computer and analytic study of the metallic liquid-glass transition [J]. *The Journal of Chemical Physics*, 1988, 88(4): 2700–2705.
- [23] TANAKA M J. Molecular dynamics study of triplet correlations in a rapidly quenched metal. I. Distribution of equilateral triplets [J]. *Journal of the Physical Society of Japan*, 1983, 52(4): 1270–1277.
- [24] WENDT H R, ABRAHAM F. Empirical criterion for the glass transition region based on monte carlo simulations [J]. *Physical Review Letters*, 1978, 41(18): 1244–1246.
- [25] YI Xue-hua, LIU Rang-su, TIAN Ze-an, HOU Zhao-yang, LI Xiao-yang, ZHOU Qun-yi. Formation and evolution properties of clusters in liquid metal copper during rapid cooling processes [J]. *Transactions of Nonferrous Metals Society of China*, 2008, 18(1): 33–39.
- [26] ZHOU L L, LIU R S, TIAN Z A, LIU H R, HOU Z Y, PENG P, LIU Q H. Microstructural evolution and martensitic transformation mechanisms during solidification processes of liquid metal Pb [J]. *Philosophical Magazine*, 2012, 92(5): 571–585.
- [27] ZHOU Li-li, LIU Rang-su, TIAN Ze-an, LIU Hai-rong, HOU Zhao-yang, ZHU Xuan-ming, LIU Q H. Formation and evolution

- characteristics of bcc phase during isothermal relaxation processes of supercooled liquid and amorphous metal Pb [J]. Transactions of Nonferrous Metals Society of China, 2011, 21: 588–597.
- [28] LIU F X, LIU R S, HOU Z Y, LIU H R, TIAN Z A, ZHOU L L. Formation mechanism of atomic cluster structures in Al–Mg alloy during rapid solidification processes [J]. Annals of Physics, 2009, 324: 32–342.
- [29] QI D W, WANG S. Icosahedral order and defects in metallic liquids and glasses [J]. Physical Review B, 1991, 44(2): 884–887.
- [30] TIAN Z A, LIU R S, LIU H R, ZHENG C X, HOU Z Y, PENG P. Molecular dynamics simulation for cooling rate dependence of solidification microstructures of silver [J]. Journal of Non-Crystalline Solids, 2008, 354: 3705–3712.
- [31] NICOLIS G, PRIGOGINE I. Self-organization in nonequilibrium systems: From dissipative structures to order through fluctuations [M]. New York: Wiley-Interscience, 1977: 115.

## 熔体初始温度对液态 $Mg_7Zn_3$ 合金凝固过程中 微观结构非线性影响的模拟研究

刘让苏<sup>1</sup>, 梁永超<sup>1</sup>, 刘海蓉<sup>2</sup>, 郑乃超<sup>2</sup>, 莫云飞<sup>1</sup>, 侯兆阳<sup>3</sup>, 周丽丽<sup>4</sup>, 彭平<sup>2</sup>

1. 湖南大学 物理与微电子科学学院, 长沙 410082;
2. 湖南大学 材料科学与工程学院, 长沙 410082;
3. 长安大学 应用物理系, 西安 710064;
4. 赣南医学院 信息工程学院, 赣州 341000

**摘 要:** 采用分子动力学方法对不同熔体初始温度对液态 Mg–Zn 合金凝固过程中微观结构演变的非线性影响进行了模拟研究, 并采用多种方法对微观结构的转变机制进行了分析。结果发现: 系统在不同熔体初始温度下以同一冷速  $1 \times 10^{12}$  K/s 凝固时, 均形成非晶态结构, 其中 1551、1541 和 1431 键型或二十面体基本原子团(12 0 12 0)对凝固微结构的转变起决定性作用; 不同熔体初始温度对凝固微结构有显著不同影响, 但这种影响只有在玻璃化转变温度  $T_g$  以下才能充分地展现出来, 非常有意义的是, 发现其影响程度的大小是与熔体初始温度的高低呈非线性变化关系, 且在一定的范围内涨落。然而, 系统的平均原子能量的变化却是与熔体初始温度成线性关系的, 即熔体的初始温度越高, 形成的非晶态结构越稳定, 即非晶形成能力越强。

**关键词:** 液态 Mg–Zn 合金; 熔体初始温度; 微观结构演变; 分子动力学模拟; 原子团类型指数法

(Edited by Hua YANG)